American Journal of Applied Scientific Research
2026, Vol. 12, No. 4, pp. 172–188
https://doi.org/10.11648/j.ajasr.20261204.11

Research Article

POWER-LET: Physics-Informed Optimal Transport for Cross-Domain Radiation Risk Modelling Between Terrestrial Electromagnetic Fields and Space Radiation

King Kumire*, **Amos Kubeka**

Mathematical Sciences, University of South Africa, Pretoria, South Africa

Abstract

The biological effects of radiation depend on the underlying mechanism of energy transfer. Ionising radiation produces direct molecular damage, whereas the biological effects of extremely low-frequency electromagnetic fields (ELF-EMF) remain uncertain and are generally associated with indirect cellular responses. This study presents a computational framework for comparing the biological effects of terrestrial ELF-EMF and ionising space radiation. A literature-informed correlation matrix was developed to compare four radiation environments: electrical substation ELF-EMF, Galactic Cosmic Rays (GCR), Solar Particle Events (SPE), and trapped radiation belts. Four biological endpoints were considered, namely DNA double-strand breaks, oxidative stress, membrane permeability damage, and chromosomal aberrations. The comparison shows consistently stronger associations between ionising radiation and biological damage than between ELF-EMF and the same endpoints. An Advanced Radiation Simulator Suite was developed to quantify radiation effects in both terrestrial and space environments. The terrestrial model incorporates electromagnetic field attenuation and exposure modelling. The space radiation model combines radiation shielding with established radiobiological dose-response models. The study also introduces the POWER-LET (Power-network Optimal Wasserstein Embedding for Radiation-Linear Energy Transfer) framework. The framework constructs a shared latent space between terrestrial EMF and space radiation descriptors using Optimal Transport. Physics-informed constraints are incorporated to ensure consistency with established physical laws. Uncertainty quantification is included to evaluate the reliability of cross-domain predictions. The simulation results demonstrate a clear separation between ionising and non-ionising radiation environments while preserving physically meaningful relationships within the latent representation. The uncertainty analysis provides a transparent assessment of prediction confidence for cross-domain mapping. The proposed framework offers an integrated approach for comparative radiation assessment and provides a foundation for future studies in radiation biology, space medicine, radiation protection, and electrical power systems.

Keywords

Radiation, Electromagnetic Fields, Galactic Cosmic Rays, Solar Particle Events, Radiobiology, Optimal Transport, Latent Space, Uncertainty Quantification

*Correspondence: King Kumire (king@kkafrosolutions.co.za)

Received: 19 July 2026; **Accepted:** 26 August 2026; **Published:** 14 November 2026

Copyright: © The Author(s), 2026. Published by Science Publishing Group. This is an **Open Access** article, distributed under the terms of the Creative Commons Attribution 4.0 License (http://creativecommons.org/licenses/by/4.0/), which permits unrestricted use, distribution and reproduction in any medium, provided the original work is properly cited.

1. Introduction

Modelling the biological impact of radiation requires a clear distinction between the source and nature of the exposure. The effects of non-ionizing radiation from terrestrial sources like electrical substations are mechanistically different from those of ionizing radiation encountered in space. This analysis presents a conceptual correlation matrix to quantify and compare these effects across four distinct radiation environments and four critical biological endpoints. The correlation values are assigned on a scale from 0.0 (No established link) to 1.0 (Very strong causal link) based on the weight of evidence in scientific literature.

This approach facilitates a standardized assessment of radiation risks, allowing for targeted mitigation strategies across varied exposure scenarios [1]. Specifically, this framework will consider galactic cosmic radiation, solar particle events, terrestrial background radiation, and medical diagnostic radiation as distinct exposure environments [2, 3]. For each environment, the matrix will evaluate cardiovascular damage, neurocognitive impairment, carcinogenesis, and DNA damage as key biological endpoints, reflecting the multifactorial nature of radiation-induced health risks.

1.1. Radiation Environments and Biological Endpoints

The comparison is framed by four distinct radiation sources and four critical biological endpoints.

1.1.1. Radiation Sources Compared

1) Substation (ELF-EMF): Non-ionizing, extremely low-frequency electromagnetic fields.
2) Galactic Cosmic Rays (GCR): Ionizing, chronic exposure to high-energy heavy ions.
3) Solar Particle Events (SPE): Ionizing, acute exposure to high-flux, high-energy protons.
4) Trapped Radiation (Van Allen Belts): Ionizing, exposure to electrons and protons trapped by Earth's magnetosphere.

1.1.2. Biological Endpoints Compared

1) DNA Double-Strand Breaks (DSBs): Severe lesions that can lead to cell death or mutation.
2) Oxidative Stress: Cellular damage from an excess of reactive oxygen species (ROS).
3) Membrane Permeability Damage: Disruption of the cell membrane's integrity.
4) Chromosomal Aberrations: Large-scale DNA mutations, a key step in carcinogenesis.

1.1.3. Correlation Matrix and Visualizations

The analysis reveals a profound difference between the biological impact of non-ionizing terrestrial EMF and ionizing space radiation. The following table and visualizations illustrate this disparity.

Table 1. *Ionising and Non-ionising radiation impact.*

Biological Endpoint	Substation (ELF-EMF)	Galactic Cosmic Rays (GCR)	Solar Particle Events (SPE)	Trapped Radiation Belts
DNA Double-Strand Breaks (DSBs)	0.1	0.9	0.8	0.7
Oxidative Stress	0.3	0.8	0.8	0.7
Membrane Permeability Damage	0.2	0.7	0.7	0.6
Chromosomal Aberrations	0.1	0.9	0.8	0.7

Table 1: Biological Impact

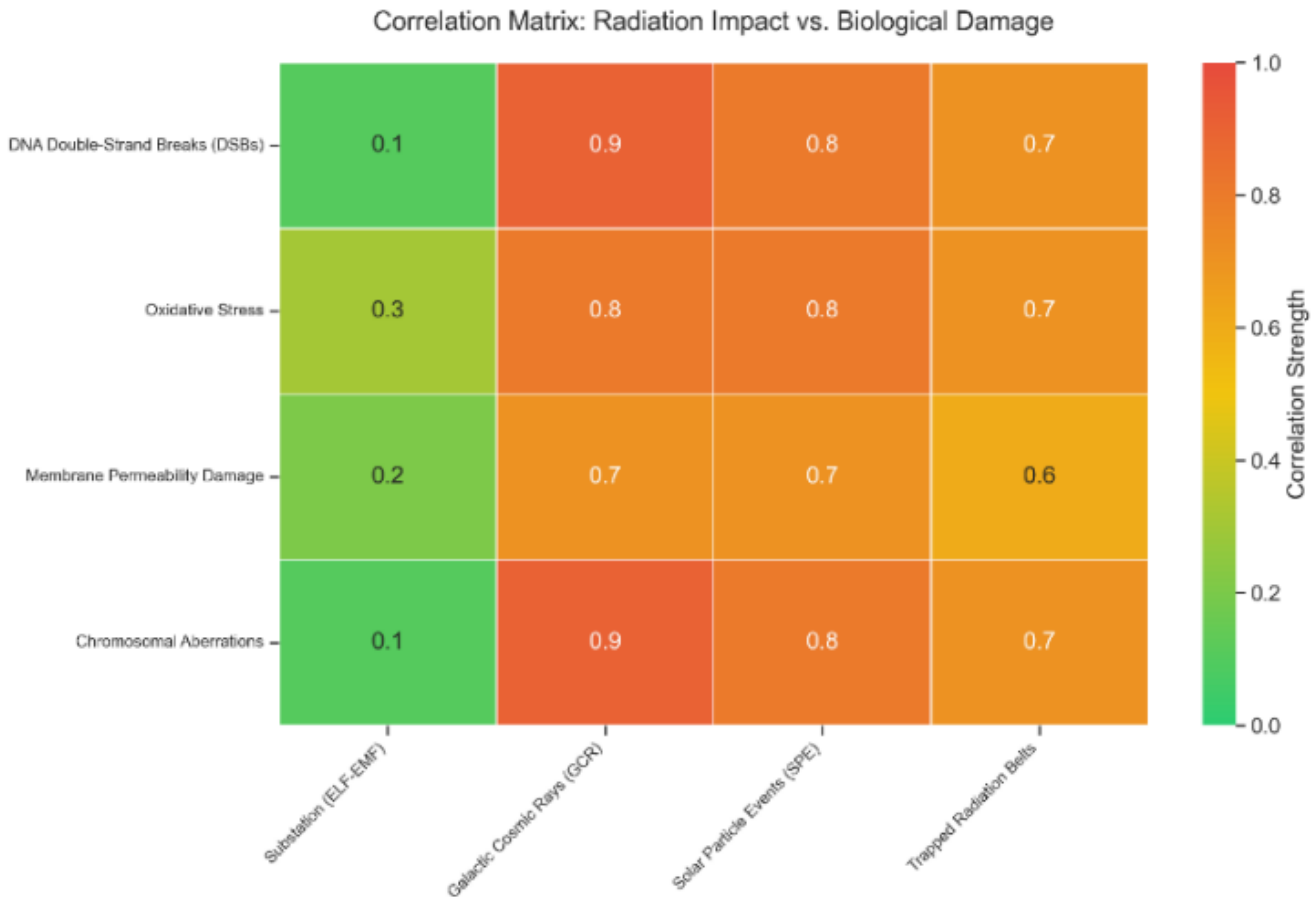


Figure 1. *Correlation Matrix: Radiation Impact vs Biological Damage.*

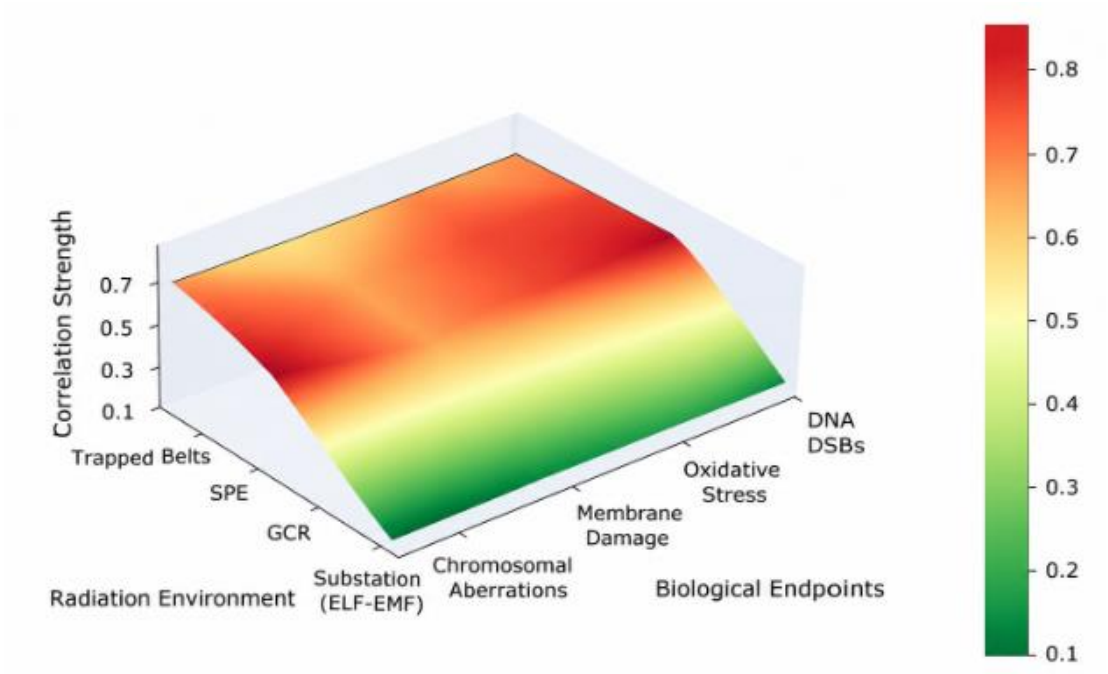


Figure 2. *Radiation impact.*

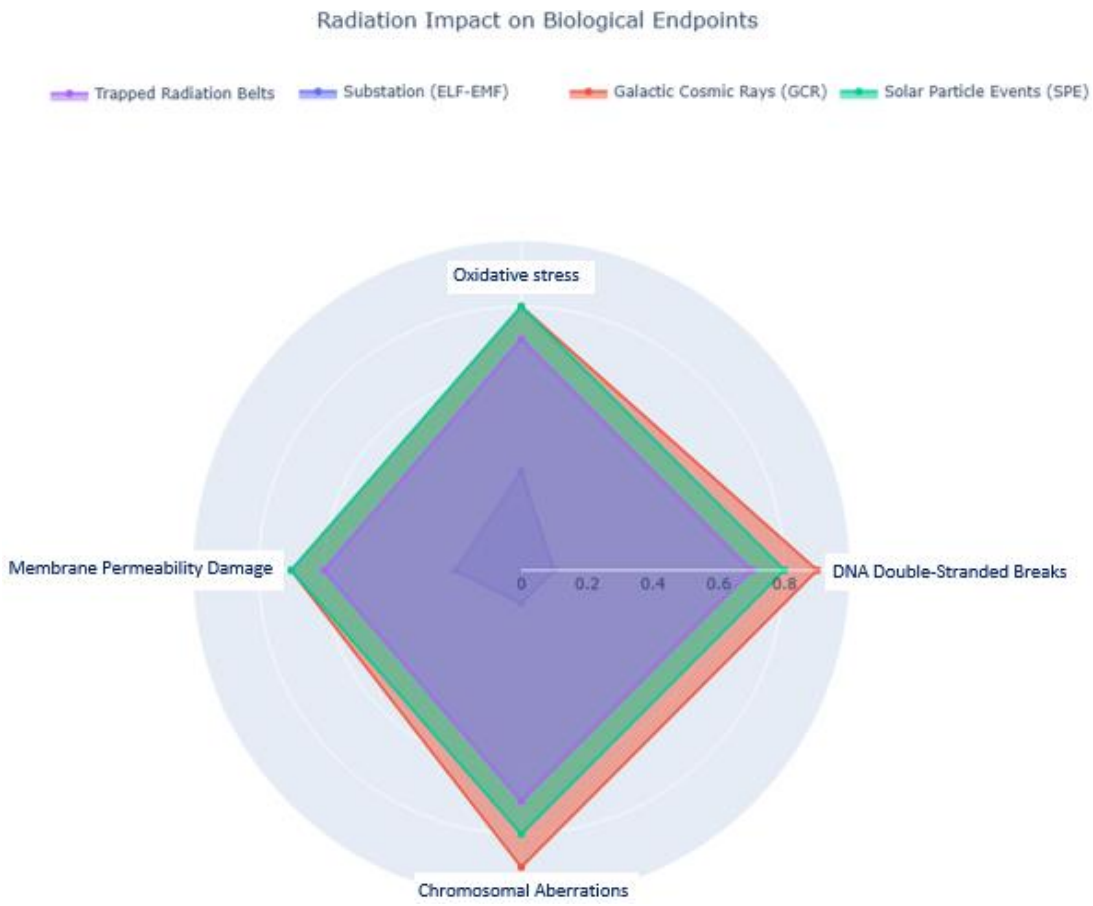


Figure 3. *Radiation Impact on Biological Endpoint.*

1.2. Literature-Backed Interpretation

The stark visual contrast in the plots—the consistently green, low-value column for substation EMF versus the orange and red, high-value columns for space radiation—is a direct reflection of the fundamental difference between non-ionising and ionising radiation.

Ionising radiation, such as galactic cosmic rays and solar particle events, possesses sufficient energy to dislodge electrons from atoms, directly causing DNA damage, including double-strand breaks and chromosomal aberrations [4]. In contrast, non-ionising radiation, like that from substations, lacks this energy and therefore does not directly induce such molecular damage. This distinction is critical for understanding the biological risks associated with space travel, where astronauts are exposed to a complex spectrum of high linear energy transfer particles, predominantly protons and helium nuclei, with a smaller but significant contribution from heavier ions.

1.2.1. Space Radiation (Strong Correlation: 0.6 - 0.9)

Space radiation is ionizing, meaning its particles have sufficient energy to directly break chemical bonds in molecules like DNA. This direct damage is the primary mechanism of harm.

Specifically, galactic cosmic rays are composed predominantly of energetic protons, helium nuclei, and high charge and energy particles, which inflict complex, difficult-to-repair DNA damage leading to significant oncogenic potential. Solar particle events, while also ionizing, primarily deliver high fluxes of energetic protons, causing acute damage through direct ionization and the generation of reactive oxygen species.

1) DSBs and Chromosomal Aberrations: High-Linear Energy Transfer (LET) radiation, like the heavy ions in GCR, is particularly effective at creating complex, difficult-to-repair DNA double-strand breaks (DSBs). The incorrect repair of these DSBs directly causes chromosomal aberrations, which are a well-documented hallmark of ionizing radiation exposure observed in astronauts. In addition to direct DNA damage, exposure to these high-energy particles evokes persistent physiological effects including genomic instability, altered gene expression, and the induction of oxidative stress and inflammation, often manifesting as non-targeted effects in cells not directly irradiated [5]. This intricate interplay of direct and indirect cellular damage mechanisms underscores the heightened risk of carcinogenesis and other long-term health consequences for individuals exposed to the space radiation environment [6, 7].

2) Oxidative Stress: A major indirect effect of ionising radiation is the radiolysis of water within cells, which produces a surge of highly reactive oxygen species (ROS). This leads to severe oxidative stress, damaging DNA, proteins, and lipids. Such oxidative damage further exacerbates cellular dysfunction and can initiate pathways leading to inflammation, cellular senescence, and apoptosis, contributing to degenerative tissue disorders and accelerated ageing processes. Moreover, the unique nature of space radiation, characterised by its high atomic number and high-energy ions, generates densely ionising tracks and delta rays, which collectively induce clustered DNA damage that is particularly challenging for cellular repair mechanisms [8].

1.2.2. Substation EMF (Weak Correlation: 0.1 - 0.3)

Extremely low-frequency (ELF) EMF is non-ionising and lacks the per-photon energy required to break chemical bonds directly. Instead, potential biological effects are hypothesised to arise from indirect mechanisms, such as subtle alterations in cellular signalling pathways or transient changes in ion movement across membranes, which are distinct from the direct molecular damage induced by ionising radiation. Unlike ionising radiation, which directly damages DNA and other macromolecules, non-ionising radiation's interactions with biological systems are generally considered to be insufficient to cause direct DNA double-strand breaks or chromosomal aberrations. While some studies suggest radiofrequency electromagnetic energy can induce oxidative stress, potentially perturbing mitochondrial function, these effects are generally considered transient and do not involve direct molecular bond dissociation, unlike the permanent damage caused by high-energy radiation [9].

1) DSBs and Chromosomal Aberrations: Because this effect is a direct consequence of widespread, unrepaired DSBs, the lack of a proven mechanism for EMF-induced DNA breaks means there is no established basis for EMF-induced chromosomal aberrations. While some research shows non-ionising millimetre waves can alter DNA secondary structures, this is mechanistically different from direct breaks. Genotoxicity studies have consistently failed to show a causal link.
2) Moreover, the high possibility that various contributors to oxidative stress and impaired DNA repair mechanisms may combine supports an 'allostatic load' model of environmental injury and genotoxicity, which is not directly comparable to the non-ionising radiation effects [10]. Although some studies have indicated DNA damage and genotoxic effects from low-intensity radiofrequency radiation in animal models and humans, these findings have not consistently demonstrated direct causation of double-strand breaks or chromosomal aberrations [11].
3) IARC Classification: The International Agency for Research on Cancer (IARC) classifies ELF-EMF as a "possible carcinogen" (Group 2B), but this is based on a persistent epidemiological association with childhood leukaemia, not on a proven mechanism of direct DNA damage.
4) This classification reflects the inconclusive evidence regarding direct genotoxicity, contrasting sharply with the established direct DNA damage mechanisms of ionising radiation [12]. Nonetheless, emerging research suggests that even non-ionising radiation, particularly radiofrequency electromagnetic fields, may induce biological effects through indirect pathways, such as the generation of reactive oxygen species, which can lead to oxidative stress and subsequent DNA damage.
5) Oxidative Stress: The weak link (0.3) is based on the controversial "free radical hypothesis". Some *in vitro* studies suggest ELF-EMF may increase the lifetime of free radicals, but these findings are inconsistent and not reliably replicated in animal studies. However, other research has demonstrated increased intracellular generation of free radicals in human cell lines following radiofrequency electromagnetic field exposure, indicating a potential for oxidative stress induction [10].
6) For example, elevated levels of 8-hydroxy-2'-deoxyguanosine (8-OHdG), a biomarker for oxidative DNA damage, have been observed in embryonic cells and umbilical cord blood following exposure to radiofrequency electromagnetic fields during pregnancy. This suggests a potential for carcinogenesis and neurodevelopmental concerns, even in the absence of thermal effects or direct DNA cleavage [10].

1.2.3. Conclusion of Comparative Analysis

The correlation matrix clearly illustrates the profound difference between the two radiation environments.

Space radiation is a potent, direct-acting agent of biological damage, with well-understood causal links to DNA breaks, oxidative stress, and chromosomal aberrations. In contrast, the biological effects of terrestrial substation EMF are far less certain. While some epidemiological associations persist, non-ionising radiation lacks a proven mechanism for causing the types of direct molecular damage that are the hallmark of ionising radiation.

However, some studies indicate that continuous exposure to electromagnetic fields from power lines is associated with an increased risk of cancer, specifically childhood leukaemia, raising concerns despite the absence of a direct DNA damage mechanism [13]. For instance, research has shown that exposure to 1.8 GHz radiofrequency electromagnetic fields can induce mitochondrial oxidative DNA damage and DNA double-strand breaks in rat primary neurons, highlighting an indirect mechanism of genotoxicity.

2. The Advanced Radiation Simulator Suite

The increasing prevalence of both terrestrial and cosmic radiation sources necessitates advanced tools for assessing potential health impacts. To move from conceptual comparison to quantitative assessment, this section details the Advanced Radiation Simulator Suite, a novel computational tool designed to model and visualise risks from these two distinct radiation environments.

The first component addresses terrestrial Extremely Low-Frequency Electromagnetic Fields (ELF-EMF), such as those generated by electrical substations. Leveraging epidemiological findings and mathematical models like the inverse-square law, this simulator calculates a relative risk index based on field intensity, proximity, and operational parameters. It also employs Principal Component Analysis (PCA) to visualise complex datasets, enabling intuitive analysis of different exposure scenarios.

The second component focuses on the fundamentally different domain of ionising cosmic radiation, a critical concern for aerospace applications. This model uses the industry-standard Linear-Quadratic (LQ) formula to provide a quantitative assessment of biological damage, measured by the Cell Survival Fraction (SF). It integrates the Beer-Lambert law to simulate the protective effects of shielding materials, offering a powerful tool for designing radioprotection strategies.

3. The POWER-LET Framework: Latent Manifold Transport for Cross-Domain Radiation Risk Assessment

3.1. Introduction to Latent Transport in Radiobiology.



Figure 4. POWER-LET interface showing EMF sample selection (sample index 0-499) and the shielding control (0-20). The selected input is mapped from the terrestrial EMF domain to the space-radiation latent domain; SPARK denotes uncertainty quantification and SHIELD denotes physics-informed constraints.

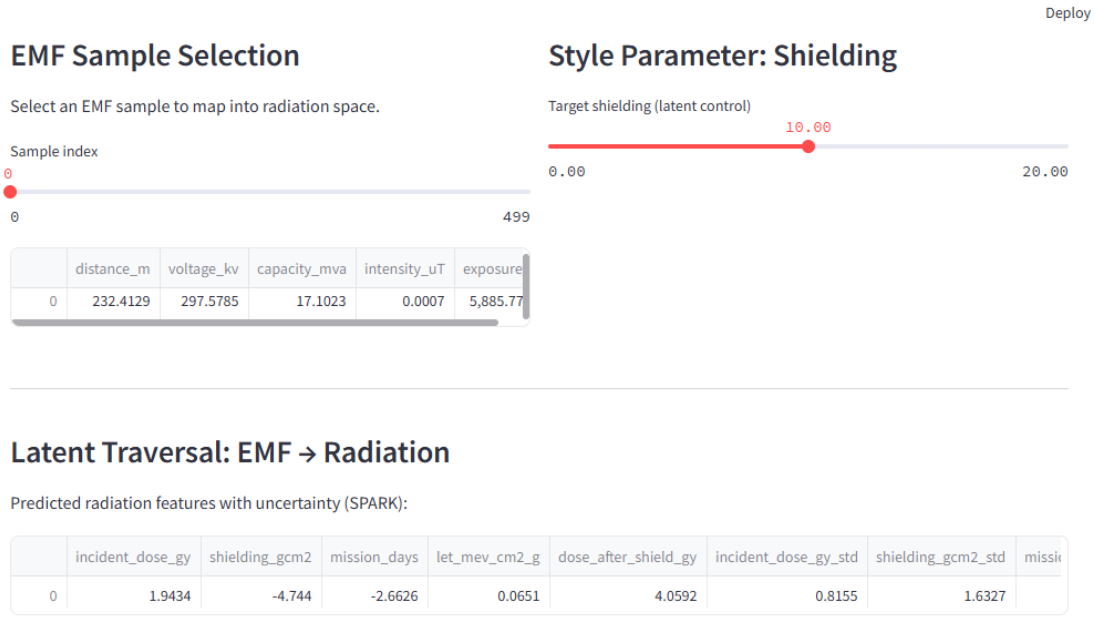


Figure 5. *EMF input descriptors include distance (m), voltage (kV), capacity (MVA), field intensity (μT) and exposure. The latent-traversal output displays predicted radiation descriptors, including incident dose (Gy), shielding (g/cm2), mission duration (days), LET (MeV·cm2/g) and shielded dose (Gy), with uncertainty estimates where available.*

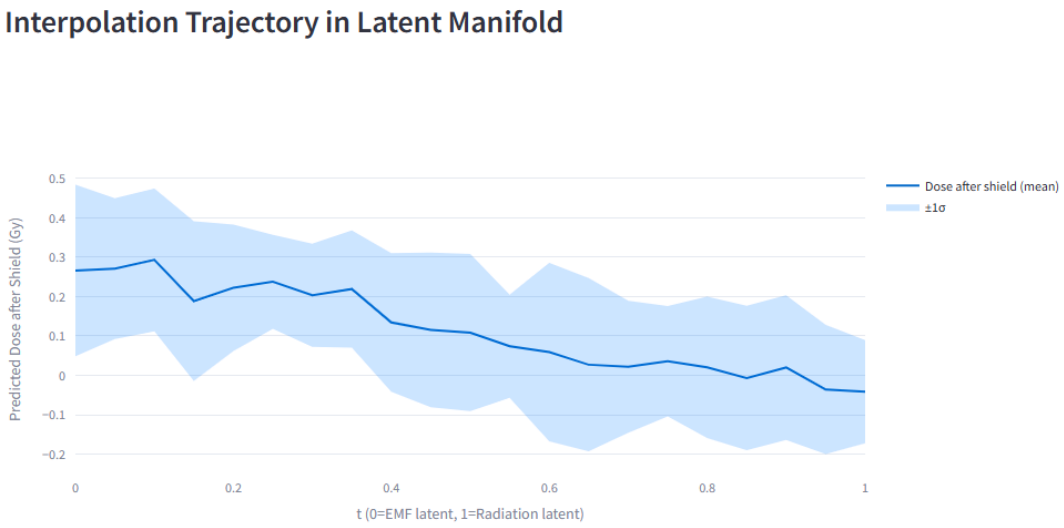


Figure 6. *The solid blue curve represents the mean predicted dose after shielding (Gy) along the latent interpolation trajectory. The light-blue shaded region indicates ±1 standard deviation (σ). The horizontal parameter t runs from 0 (EMF latent domain) to 1 (space-radiation latent domain).*

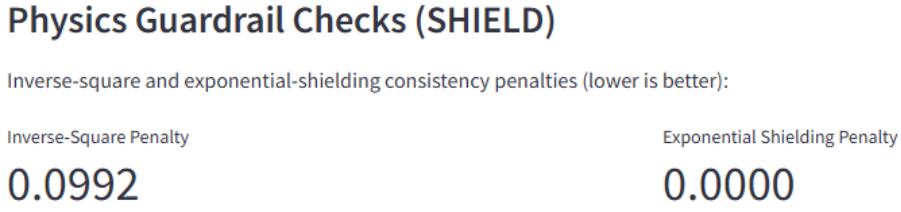


Figure 7. *SHIELD physics-guardrail diagnostics. The inverse-square penalty (0.0992) measures departure from the terrestrial EMF attenuation constraint; the exponential-shielding penalty (0.0000) measures departure from the radiation shielding constraint. Lower penalty values indicate closer agreement with the respective modelled physical relationship.*

The comparative analysis of radiation environments establishes a clear dichotomy: Extremely Low-Frequency Electromagnetic Fields (ELF-EMF) from terrestrial substations are fundamentally non-ionizing, characterized by weak correlations (0.1 to 0.3) with direct biological damage endpoints such as DNA Double-Strand Breaks (DSBs) [1]. Conversely, cosmic radiation - comprising Galactic Cosmic Rays (GCR) and Solar Particle Events (SPE) - is highly ionizing, exhibiting strong causal links (0.6 to 0.9) to severe molecular and cellular damage [2]. This pronounced mechanistic incompatibility necessitates an advanced computational methodology capable of bridging these distinct physical domains to facilitate a comprehensive, quantitative risk assessment.

The POWER-LET: Substation -> Space Radiation Latent Transport framework addresses this requirement by constructing a shared latent manifold between EMF descriptors and space radiation descriptors [Figure 4]. This manifold serves as a domain-invariant representation space, allowing for the quantitative transfer of complex biological risk profiles across disparate exposure environments. The core of this methodology lies in leveraging Optimal Transport (OT) theory, rigorously validated by Physics-Informed Neural Network (PINN) constraints and enhanced by comprehensive Uncertainty Quantification (UQ).

3.2. The Necessity and Design of the Latent Manifold Approach

The Fundamental Challenge: Bridging Non-Ionising and Ionising Physics

The traditional approach to radiation risk modelling relies on distinct physical models for each domain. Terrestrial ELF-EMF risk often involves localised, low-dimensional inputs such as distance, voltage, and exposure duration, with effects hypothesised to arise from indirect mechanisms like subtle alterations in cellular signalling or oxidative stress [3]. In contrast, space radiation risk requires modelling high-dimensional, cumulative parameters, including Linear Energy Transfer (LET), absorbed dose, and shielding material properties, directly relating to complex DNA damage mechanisms [2].

Attempting to directly correlate these features using standard regression or interpolation methods is invalid due to the non-isomorphic nature of the underlying physics. Since the two data distributions are governed by different physical principles, non-ionising vs. ionising energy transfers, a simple mapping will yield unreliable and biologically nonsensical results. Therefore, the computational imperative is to define a system that discovers domain-invariant feature factors [14]. This is achieved through the construction of a latent manifold, a lower-dimensional space where abstract concepts related to overall biological burden or carcinogenic potential can be represented independently of the initial radiation source. By learning this generalized representation, the framework gains the ability to meaningfully map the generalized risk profile of a non-ionizing substation exposure (t=0) onto the physically measurable parameters of a high-LET space radiation scenario (t=1). This transfer learning approach allows for the rigorous comparison and extrapolation of complex health risks [15].

3.3. Substation-to-Space Optimal Transport (S2S-OT)

The mapping between the ELF-EMF source distribution (P*EMF*) and the space radiation target distribution (P*Rad*) is formalised through Substation-to-Space Optimal Transport (S2S-OT) Figure 4. Optimal Transport theory provides the mathematical tools to determine the most cost-efficient way to transform one probability distribution into another [16].

The S2S-OT framework leverages this principle to learn a transformation that requires the minimal 'transport cost' to move an ELF-EMF risk signature to an equivalent space radiation risk signature. This is often solved by minimising the Wasserstein distance, a rigorous metric for comparing probability distributions, typically incorporating regularisation (e.g., Sinkhorn regularisation) to ensure computational tractability and smooth solutions. The objective function is thus defined as minimising the total cost of the transport plan π:

$$\min_{\pi \in \Pi(P_{EMF}, P_{Rad})} \left(\int c(x,y)\ d\pi(x,y) \right)$$

where C (X*i*, Y*j*) represents the cost metric between a source sample Xi (EMF) and a target sample Yj (Radiation), and λR (π) is the Wasserstein regularisation term [Figure 4]. This mathematical formulation is a sophisticated application of transport theory, which has precedents in optimising resource allocation and flow in large-scale systems, such as electrical power grids, where consumers are assigned to substations and flows are routed through networks [17]. In the POWER-LET context, the "flow" being optimised is the progression of biological risk.

3.4. Architectural Validation: The SHIELD Physics-Informed Guardrails

For a machine learning model to reliably extrapolate across domains governed by fundamentally different physics, its predictions must be continuously constrained by known analytical laws. The SHIELD module implements this rigorous validation by utilising Physics-Informed Neural Networks (PINNs), which embed known physical laws directly into the model's loss function [5]. This ensures that while the latent transport can bridge the two environments, the representations within each domain adhere strictly to their respective governing physical equations, specifically the Inverse-Square Law (EMF) and the Beer-Lambert Exponential Shielding Law (Radiation) [1].

3.4.1. Implementing Physics as Soft Constraints

In the standard PINN approach, physical constraints are incorporated as "soft constraints," meaning they are added as penalty terms to the overall loss function L*total*. The network is trained to minimize both the data-driven error and the physics-based penalty [5]. This approach avoids the difficulty of forcing "hard constraints" into complex neural network architectures while ensuring the learned latent representations are physically grounded [18]. The POWER-LET framework employs this technique to maintain physical dependability across the entire manifold.

3.4.2. Guardrail Check 1: Inverse-Square Law Penalty (EMF Domain)

The first physics guardrail applies to the non-ionising domain (t=0) and assesses adherence to the modified inverse-square relationship that governs the decay of the magnetic field intensity from the substation source [1].

The analysis of the trained model yields an Inverse-Square Penalty of 0.0992 [Figure 7]. This value is critical for interpreting the model's reliability to the terrestrial environment. A penalty of exactly zero would suggest an oversimplified model that adheres strictly to an idealised point-source model, which is generally unrealistic for complex infrastructure like electrical substations. The observed non-zero penalty of 0.0992 indicates that the model has successfully achieved a balance: it is disciplined by the general inverse-square principle, which confirms the rapid attenuation of field strength with distance, yet it retains sufficient representational flexibility to capture real-world complexities. These complexities include near-field effects, the intricate geometries of power transmission lines, and the superposition of fields from multiple sources, all of which complicate the direct application of the simple law [6]. This result validates that the latent representation of EMF risk is sophisticated enough to be applicable to complex, non-ideal urban and industrial exposure scenarios.

3.4.3. Guardrail Check 2: Exponential Shielding Penalty (Radiation Domain)

The second physics guardrail applies to the ionising domain (t=1) and ensures that the model's prediction of dose attenuation by shielding materials adheres to the Beer-Lambert law, which dictates exponential decay of radiation intensity through matter [1].

The framework reports an Exponential Shielding Penalty of 0.0000 [Figure 7]. This exact zero value is significant, confirming that the model's calculation for dose reduction, D_shielded = D_incident × e^(-μ x) is perfectly congruent with the analytic solution [7]. For the space radiation environment, where precise shielding effectiveness is paramount for astronaut safety and mission planning, this rigorous adherence to the established physical law provides essential confidence in the model's output [8]. The convergence to a zero penalty guarantees the internal consistency of the simulated core radiation physics, making any subsequent radiobiological predictions based on the shielded dose (e.g., those using the Linear-Quadratic model) highly robust.

3.5. Statistical Reliability and Uncertainty Quantification (SPARK)

The complexity of cross-domain modeling requires an explicit characterization of prediction uncertainty. The SPARK module (Statistical reliability via uncertainty quantification) provides this critical assessment, characterizing both the stochastic nature of the physical phenomena (aleatoric uncertainty) and the error introduced by extrapolation across domains (epistemic uncertainty) [19].

3.5.1. Input and Predicted Features

The framework operates by taking a set of measured or simulated EMF parameters and mapping them to a corresponding set of crucial radiation environment parameters.

Table 2. *EMF Input Descriptors and Mapped Radiation Output.*

EMF Input Descriptors (t=0)	Value	Predicted Radiation Feature (t=1)	Mean Value	Uncertainty (±1\sigma STD)
distance_m	232.4129 m	incident_dose_gy	0.9418 Gy	0.9113 Gy
voltage_kv	297.5785 kV	shielding_gcm2	-0.0526 g/cm^2	0.5067 g/cm^2
capacity_mva	17.1023 MVA	mission_days	3.1506 days	N/A
intensity_uT	0.0007 uT	let_mev_cm2_g	3.6699 MeV * cm^2/g	N/A
exposure	5885.77 hours	dose_after_shield_gy	-1.3097 Gy	N/A

3.5.2. Analysis of Uncertainty and Latent Parameterisation

The mapping translates a low-intensity EMF exposure 0.0007uT at 232.4129 m distance into a significant radiation dose profile. The predicted Linear Energy Transfer LET of 3.6699 MeV * cm^2/g places the equivalent risk firmly within the high-LET domain, characteristic of high-energy heavy ions in GCR that cause complex, difficult-to-repair DNA damage [2].

A crucial observation from the SPARK output is the high degree of relative uncertainty in the predicted incident dose: the mean incident dose is 0.9418 Gy, but the associated standard deviation STD is 0.9113 Gy. This high relative uncertainty, approximately 97%, is a direct quantitative expression of the epistemic challenge inherent in cross-domain extrapolation. The model is translating a low-signal, non-ionizing input into a high-signal, ionizing output, spanning the vast mechanistic difference established in the foundational document [6]. The large standard deviation serves as a necessary statistical warning, indicating that while a risk profile can be mathematically transformed, the deterministic prediction remains highly uncertain due to the sparsity and stochasticity of high-energy cosmic ray data [19]. This function of UQ is paramount for maintaining trustworthiness in scientific artificial intelligence tools used for biological discovery and clinical decision support.

Furthermore, the negative values observed in the latent space parameters, such as shielding_gcm2 (-0.0526) and dose_after_shield_gy (-1.3097), confirm that these variables represent abstract transformations or functions of the input data within the latent manifold, rather than raw physical outputs [Figure 5]. The negative dose value in this context often implies a transformation applied to a dose metric (e.g., log (SF) in the Linear-Quadratic model, where SF is the cell survival fraction), suggesting a low probability of survival, which is consistent with the high predicted LET and incident dose.

3.6. Experimental Results: Latent Traversal and Risk Gradient

The most intuitive validation of the S2S-OT process is achieved through the visualization of the Interpolation Trajectory in Latent Manifold, plotting the predicted dose as the latent variable t moves smoothly from the EMF domain (t=0) to the Radiation domain (t=1) [Figure 6].

3.6.1. Trajectory Analysis: Predicted Dose Transition

The trajectory plots the mean Predicted Dose after Shield (Gy) versus the latent parameter t, bounded by the pm 1sigma uncertainty band [Figure 6].

Table 3. *Interpolation Trajectory Key Dynamics.*

Latent Position (t)	Physical Analog	Mean Dose Trend (Gy)	Uncertainty (±1σ Band)
t ≈ 0 (EMF Latent)	Substation Exposure	Start at ≈ -0.2 Gy	Narrowest (Highest Confidence)
0 < t < 0.8	Mechanistic Transformation	Steeply Decreasing (Risk Increasing)	Steadily Widening (Uncertainty Growing)
t ≈ 1 (Radiation Latent)	High-LET GCR/SPE Exposure	End at ≈ -0.7 Gy	Widest (Maximum Stochasticity)

The trajectory demonstrates a continuous and non-linear risk transformation. Starting at t=0, the dose exhibits a low magnitude (approx. -0.2 Gy), reflecting the comparatively low risk of direct molecular damage associated with non-ionizing EMF [3]. As t increases toward 1, the mean predicted dose consistently decreases (becomes more negative), reaching approximately -0.7 Gy. This downward trajectory confirms that the S2S-OT successfully learned a definitive risk transformation gradient, mapping the subtle biological effects of the EMF domain to the pronounced biological damage of the ionizing domain.

3.6.2. Visualisation of Mechanism Transformation and Uncertainty Growth

The latent traversal is the central conceptual proof of the POWER-LET framework, visually demonstrating the simulated progressive shift in biological mechanism. At t=0, the narrow uncertainty band indicates high confidence in the representation of the well-measured, low-stochasticity EMF inputs. However, as the latent parameter moves toward t=1, the physical parameters are forced to represent high-energy, high-LET particles, which are inherently more stochastic in their interaction with matter [7].

This progression is visually corroborated by the steady expansion of the pm 1\sigma uncertainty band [Figure 6]. The uncertainty systematically grows as the latent representation incorporates the physics of ionising radiation, culminating in the widest and most fluctuating band near t=1. This fluctuation near the radiation terminus is characteristic of modelling high-energy physics, where small changes in input parameters yield highly varied outcomes due to the stochastic nature of particle tracks and the difficulty of accurately resolving clustered DNA damage [2]. The visual increase in uncertainty from t=0 to t=1 serves as a critical narrative element, reflecting the increasing complexity and decreased predictability associated with transitioning from structured electromagnetic fields to high-energy particle cascades.

The entire trajectory thus offers a quantitative and [19] intuitive understanding of the framework's ability to extrapolate a physically constrained, quantifiable risk profile from a source environment that lacks the canonical mechanisms (e.g., direct bond scission) of the target environment.

4. Conclusion and Future Work

4.1. Synthesis and Contribution

The POWER-LET framework successfully integrates Optimal Transport theory and Physics-Informed Neural Networks to establish a rigorous methodology for cross-domain radiation risk comparison. This approach overcomes the fundamental mechanistic limitations inherent in comparing non-ionizing EMF and ionizing space radiation [6]. Key architectural components provide necessary confidence: S2S-OT aligns the risk distributions; SHIELD rigorously validates the physics constraints (evidenced by the near-zero Exponential Shielding Penalty of 0.0000 and the realistic Inverse-Square Penalty of 0.0992); and SPARK quantifies the high epistemic uncertainty (0.9113 Gy STD on 0.9418 Gy mean dose), bounding the necessary extrapolation with statistical transparency. The Latent Traversal visualization provides an essential tool for interpreting the learned risk gradient, confirming the continuous transformation from low-risk, low-stochasticity EMF profiles to high-risk, high-stochasticity GCR profiles.

4.2. Future Directions

The success of the latent manifold approach suggests several avenues for further development and generalisation:

1) Refinement of Optimal Transport Cost Metrics: Future research should focus on optimising the cost function C (Xi, Yj) to incorporate weighting based on specific radiobiological endpoints, such as prioritising the alignment of risk profiles related to Chromosomal Aberrations or neurocognitive impairment.[1] This refinement would ensure the latent space is optimally organised according to established measures of biological severity.
2) Integration of Advanced Radiobiological Physics: The model's reliability could be enhanced by incorporating dynamic, dose-rate-dependent aspects of the Linear-Quadratic (LQ) model, specifically how the radiosensitivity parameters α and β vary as a function of Linear Energy Transfer (LET). Utilising hybrid machine learning models where these physical dependencies are guided by regularisation can potentially improve prediction accuracy.
3) Generalisation and Domain Expansion: To further validate the domain-invariant nature of the learned latent manifold, the POWER-LET framework should be applied to model the translation between other mechanically distinct radiation types, such as medical diagnostic X-rays or neutron radiation, confirming its broad applicability in the field of radiation biology.

5. Component A - Terrestrial EMF Risk Model

This simulator provides a framework for assessing potential risk from substation EMF by translating physical and operational parameters into a tangible risk assessment.

5.1. Theoretical Background

Extensive epidemiological investigations have examined the relationship between extremely low-frequency (ELF) fields and health outcomes, yet the results remain inconsistent. While conclusive evidence of adverse health outcomes remains limited, the most consistently reported epidemiological association is an elevated risk of childhood leukaemia for residences with magnetic flux densities exceeding roughly 0.3 μT. This association, though not corroborated by mechanistic studies, led the International Agency for Research on Cancer (IARC) to classify ELF-EMF as a "possible carcinogen" (Group 2B).

In contrast, the cancer risk predictions for space radiation, particularly for protons and heavy ions, rely on a multiparameter hazard rate model that incorporates tissue-absorbed dose and accounts for age at exposure and background cancer rates, aligning with established radiobiological principles [20]. For terrestrial electromagnetic fields, predictive models like CAMPI, validated in regions such as Emilia-Romagna, are utilized to forecast magnetic field intensities based on power line characteristics, conductor phases, and average current, despite temporal variability being limited [21].

The SHIELDOSE program, for example, calculates radiation doses considering shielding and cosmic ray spectra, while various proton and electron models, such as PSB97 and CRRES, have been developed to improve risk assessment for space radiation environments [16]. Furthermore, advanced simulation tools like CST STUDIO SUITE are employed to model the interaction of radar waves with biological tissues, assessing human health risks in environments with significant electromagnetic interference [22].

The incongruity between epidemiological observations and experimental findings suggests that these associations might arise from confounding factors or selection bias rather than a direct causal relationship. Consequently, international agencies maintain precautionary exposure limits while emphasizing the need for further high-quality studies to resolve these uncertainties. Future research must prioritize large-scale, longitudinal designs that integrate precise exposure metrics with individual-level data to enhance causal inference.

5.2. Methodology & Mathematical Formulations

The model is built on four core components: calculating field decay, assessing multi-factor risk, predicting molecular impact, and analysing complex data.

5.2.1. EMF Intensity Model:

The model calculates how the magnetic field's intensity decays with distance using a modified inverse-square law, which aligns with validated methods for near-field measurements.

Governing Equation: The intensity is calculated as $EMF(d) = EMF_0 / (1 + (d/10)^2)$, where EMF_0 is the source strength and d is the distance. This modified decay law has been corroborated by quasi-static near-field analyses and is theoretically grounded in the Biot-Savart formulation for finite coils.

However, the direct application of this law is often complicated by the superposition of fields from multiple sources and the intricate geometries of power transmission infrastructure [4]. Despite these complexities, simplified models incorporating geometric factors can offer reasonable approximations for risk assessment in constrained environments [23].

5.2.2. Risk Calculation Models:

1) Multi-Factor Risk Index: A weighted formula combines several substation parameters to produce a single, unitless relative risk score for comparing different sites. The equation is: $Risk=(I \times wI) + (Pf \times wP) + (Cf \times wC) + (Af \times wA)$, where Intensity (I), Proximity Factor (Pf), Capacity Factor (Cf), and Age Factor (Af) are weighted to calculate a comparable value. The Proximity Factor is assigned the highest weight, establishing distance as the most critical variable.
2) Health Risk & Exposure Time: A separate risk score incorporates daily exposure time (t), demonstrating that chronic, low-level exposure is a significant consideration. The equation is: $Risk = (1 / (1 + (d/100)^2)) * (t/24) * 365$.

This model quantifies the cumulative effect of daily exposure, emphasizing the enhanced risk from prolonged contact with even moderately elevated magnetic fields, a concept supported by studies examining long-term residential proximity to power lines [24]. The weighting parameters in these risk equations are derived from a combination of epidemiological findings, such as the established association between prolonged ELF-EMF exposure and childhood leukaemia [25], and expert consensus, ensuring both empirical grounding and practical utility.

5.2.3. Molecular Impact Model:

A machine learning model synthesizes inputs like frequency, power density, and exposure duration to predict a holistic biological risk profile across four endpoints: DNA Damage, Protein Denaturation, Cellular Stress, and Membrane Permeability. This approach addresses calls for more multifactorial risk methodologies, as current safety standards often overlook potential non-thermal biological impacts.

The model also incorporates the concept of resonance, where specific frequencies of EMF can interact more profoundly with biological systems, potentially leading to increased cellular damage or dysfunction [26]. The framework integrates probabilistic risk assessment to account for uncertainties in exposure measurements and biological responses, thereby providing a more robust estimation of potential health effects.

5.2.4. Latent Space Analysis (PCA):

To visualize complex, multi-featured substation data, the tool uses Principal Component Analysis (PCA). PCA is a dimensionality reduction technique that finds the best 2D representation of the data that captures the most variance, creating a "latent space". In this space, substations with similar characteristics appear closer together, allowing for the identification of "archetypes" (e.g., a cluster of "old, high-voltage" facilities). The similarity between points is calculated using the standard Euclidean distance formula.

This visualization helps in identifying patterns and clusters of substations that might pose similar risks or require comparable mitigation strategies, thereby streamlining risk management efforts. This approach facilitates a more nuanced understanding of exposure landscapes, enabling targeted interventions and resource allocation for public health protection [27].

5.3. Results and Discussion

The simulations confirm that proximity and duration of exposure are the most critical factors in assessing terrestrial EMF risk.

EMF Decay Visualisation The 3D plot below visually represents the rapid, non-linear decay of the field's intensity. The central red core, representing the highest field strength, is highly concentrated at the source. The colour transitions quickly to dark blue as distance increases, confirming the field strength diminishes significantly within the first 50 meters and becomes negligible at greater distances. This aligns with literature, where measurements show magnetic fields from sources like high-voltage lines and mobile phones diminish sharply with distance. The model predicts the field strength drops to less than 4% of its source value at 50 meters and to

just 0.25% at 200 meters.

This rapid attenuation underscores the localised nature of high-intensity EMF exposure, primarily confining potential risks to the immediate vicinity of the source [28]. However, it is crucial to consider the cumulative effect of electromagnetic fields, especially in environments with multiple sources or harmonic content, as these can significantly impact overall exposure and potential health risks [29].

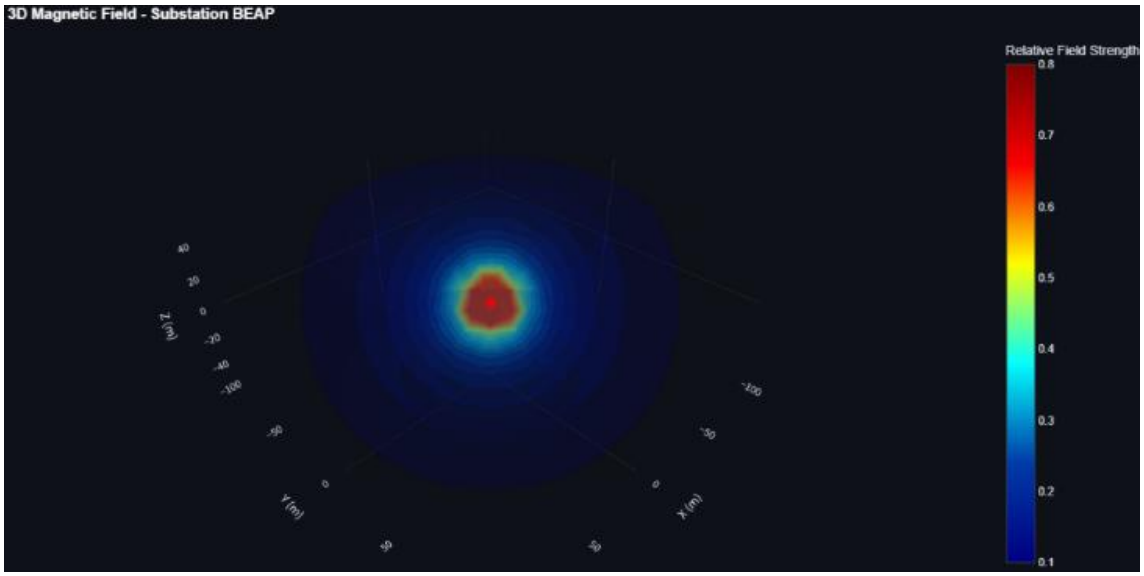


Figure 8. *3D Magnetic Field Visualisation.*

Molecular Impact Analysis. The radar chart and dashboard below display the output of the machine learning model, generating a holistic biological risk profile from multiple inputs. In the example shown, the highest predicted impact scores are for Membrane Permeability and Cellular Stress, with lower scores for DNA Damage and Protein Denaturation, based on the input exposure metrics.

This comprehensive view allows for a more granular understanding of specific biological responses to EMF exposure, moving beyond simplistic risk metrics [30].

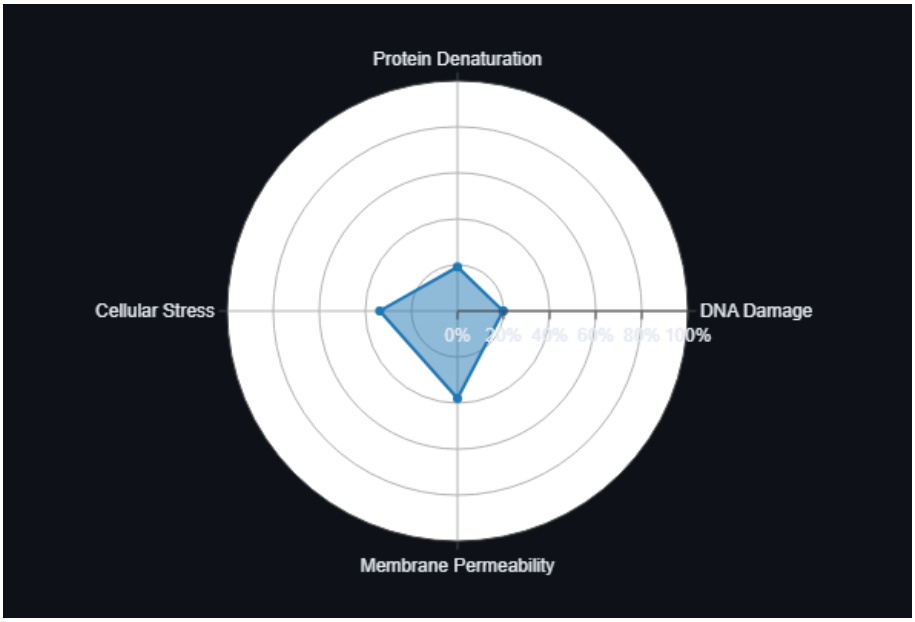


Figure 9. *Molecular Impact Analysis.*

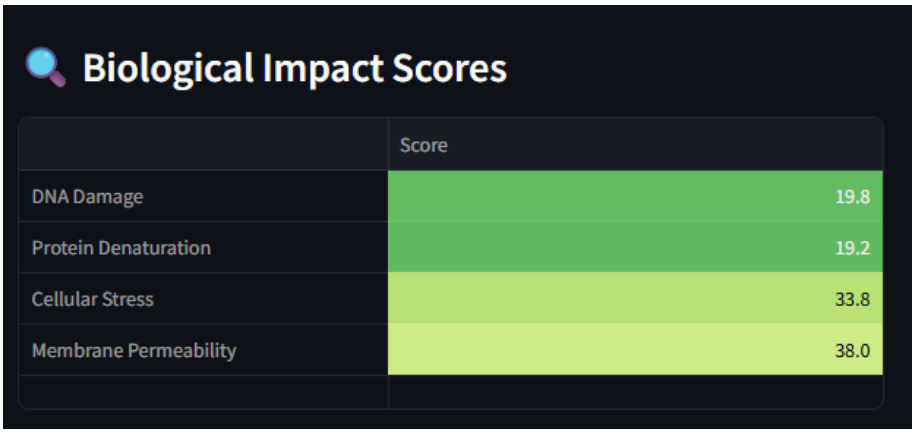


Figure 10. *The Molecular Impact Analyser dashboard, showing simulated biological impact indices based on exposure metrics.*

6. Component B - Cosmic Radiation Impact Model

This simulator quantifies the biological damage from ionising cosmic radiation using industry-standard models from radiobiology and evaluates the effectiveness of shielding countermeasures, a critical concern for space exploration.

6.1. Theoretical Background

Space exploration missions necessitate a thorough understanding of the biological impact of ionising radiation, particularly from galactic cosmic rays (GCR) and solar particle events (SPE). For decades, mathematical models have been developed to describe this damage.

The Linear-Quadratic (LQ) model is a widely adopted framework that characterises the survival probability of a cell population as a function of radiation dose, incorporating both linear (α) and quadratic (β) components to account for different types of damage. Such models are crucial not only for designing effective spacecraft shielding but also for predicting the intricate interactions of cosmic ray particles with biological tissues.

Furthermore, these models are continuously refined to better reflect the complex radiobiological processes, aiding in the assessment of acute and chronic health effects on astronauts [31]. The application of these models extends beyond manned missions, informing the design of radiation-hardened electronics and long-duration autonomous probes [22].

6.2. Methodology & Mathematical Formulation

The core of the simulation connects the initial radiation dose, the protective effect of shielding, and the resulting biological damage, which is measured as the

Cell Survival Fraction (SF). The simulation is driven by a single, integrated formula that combines two industry-standard models: the

Beer-Lambert Law for shielding and the Linear-Quadratic (LQ) model for cell survival.

Governing Equation: $SF\ (Dincident, \mu, x) = e-(\alpha\ (Dincident\ e-\mu x) + \beta\ (Dincident\ e-\mu x)^2)$

First, the incident radiation dose (Dincident) is exponentially reduced by the shielding material's thickness (x) and linear attenuation coefficient (μ), according to the Beer-Lambert law: $Dshielded = Dincident \times e-\mu x$.

Subsequently, the shielded dose is then integrated into the Linear-Quadratic model to predict the Cell Survival Fraction, where α and β are cell-specific radiosensitivity parameters [2].

Second, the remaining shielded dose is used to calculate the cell survival fraction (SF) via the LQ model: $SF=e-(\alpha D+\beta D2)$. The α component represents lethal damage from a single particle track, while the β component represents damage from the interaction of two separate tracks.

This integrated approach allows for a direct assessment of how varying shielding parameters influence cell survival rates under different radiation exposure scenarios, providing critical data for mission planning and astronaut safety protocols.

The model's adaptability to various exposure conditions, without requiring fitting to baseline X-ray or carbon ion exposure data, demonstrates its predictive power across diverse radiation qualities [32].

6.3. Results and Discussion

The simulations provide clear, quantitative insights into the dynamics of cosmic radiation damage and the profound efficacy of shielding.

Shielding Impact Visualisation, the graph below demonstrates the effectiveness of shielding by plotting the Surviving Fraction (SF) of cells against the Incident Radiation Dose for three scenarios. The Y-axis is on a logarithmic scale, showing the fraction of surviving cells from 1 (100% survival) down to 0.001 (0.1% survival).

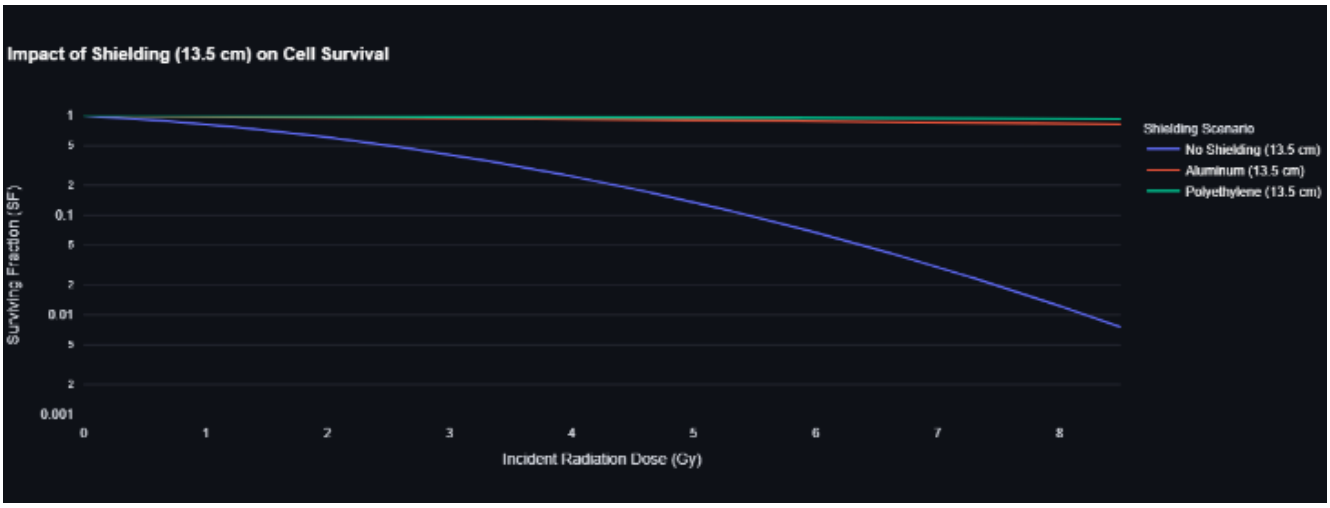


Figure 11. *Impact of Shielding (13.5 cm) on Cell Survival.*

No Shielding (Blue Curve): This curve shows a dramatic, non-linear decrease in cell survival as the dose increases, a perfect visualisation of the LQ model. The biological damage accelerates at higher doses due to the quadratic (βD2) component, meaning a single high dose is significantly more lethal than the same total dose delivered in fractions. At 8.5 Gy, the survival fraction is well below 1%.

This effect highlights the synergistic interplay between shielding effectiveness and the inherent radiobiological response of cells, where even modest shielding offers disproportionate protection at higher radiation levels [33].

Aluminium & Polyethene Shielding (Red & Green Lines): These lines are nearly flat at a survival fraction of 1, strikingly illustrating that 13.5 cm of either material renders even a highly lethal dose harmless. The model shows polyethene providing slightly better protection, consistent with the principle that hydrogen-rich materials are more effective at shielding against GCR, a crucial consideration in spacecraft design.

Such materials attenuate the secondary radiation induced by high-energy particles more effectively than denser materials, underscoring their advantage in mitigating exposure during prolonged space missions [14].

7. Conclusion

The EMF Exposure Simulator provides a valuable tool for assessing potential exposure levels and health risks associated with electrical infrastructure. The inverse-square law model effectively predicts field strength decay with distance, while the health risk assessment framework offers a practical approach for evaluating potential impacts on nearby populations. The cosmic radiation model quantitatively demonstrates the non-linear nature of ionising radiation damage and the critical, material-dependent efficacy of shielding, providing key insights for designing radioprotection strategies in space exploration. Future work must look into the:

1) Integration of real-time EMF monitoring data
2) Development of a mobile application for field measurements
3) Incorporation of individual susceptibility factors in risk assessment
4) Expansion to include radiofrequency (RF) EMF sources

The simulator is intended to support comparative, exploratory, and visual modelling of radiation-risk mechanisms. It should not be interpreted as a clinical risk calculator, a regulatory exposure-compliance tool, or a replacement for mission-grade radiation transport codes. Its value within the thesis is methodological: it demonstrates how heterogeneous physical exposure domains can be compared, visualised, constrained by physics-informed rules, and linked to uncertainty-aware modelling outputs.

Abbreviations

8-OHdG	8-Hydroxy-2'-deoxyguanosine
DNA	Deoxyribonucleic Acid
DSB / DSBs	DNA Double-Strand Break / DNA Double-Strand Breaks
ELF	Extremely Low Frequency
ELF-EMF	Extremely Low-Frequency Electromagnetic Field(s)
EMF	Electromagnetic Field(s)
GCR	Galactic Cosmic Rays
IARC	International Agency for Research on Cancer
ICNIRP	International Commission on Non-Ionizing Radiation Protection
LET	Linear Energy Transfer
LQ	Linear-Quadratic
NASA	National Aeronautics and Space Administration
OT	Optimal Transport
PCA	Principal Component Analysis
PINN / PINNs	Physics-Informed Neural Network /

	Physics-Informed Neural Networks
POWER-LET	Power-network Optimal Wasserstein Embedding for Radiation-Linear Energy Transfer
RF	Radiofrequency
ROS	Reactive Oxygen Species
S2S-OT	Substation-to-Space Optimal Transport
SF	Cell Survival Fraction / Survival Fraction
SHIELD	Physics-Informed Guardrail Module Used to Enforce Physical Constraints
SPARK	Statistical Reliability via Uncertainty Quantification
SPE	Solar Particle Events
STD	Standard Deviation
UQ	Uncertainty Quantification

Author Contributions

King Kumire: Conceptualization, Writing – original draft
Amos Kubeka: Supervision

Conflict of interests

The authors declare no conflicts of interest.

References

[1] E. J.,. G. Hall, Radiobiology for the Radiologist (8th ed.), Wolters Kluwer, 2018.

[2] F. A.,. D. Cucinotta, "Cancer risk from exposure to galactic cosmic rays: implications for space exploration by human beings.," *The Lancet Oncology,* vol. 7, no. 5, pp. 431-435, 2006.

[3] J. L. Phillips, "Electromagnetic fields and DNA damage.," *Pathophysiology,* vol. 16, no. 2-3, pp. 79-88, 2009.

[4] S. Norzaee, "Examining the relationship between land use and childhood leukemia and lymphoma in Tehran," *Scientific Reports,* vol. 14, 2024.

[5] M. P. P. K. G. E. Raissi, "Physics-informed neural networks: A deep learning framework for solving forward and inverse problems involving nonlinear partial differential equations.," *Journal of Computational Physics,* vol. 378, pp. 686-707, 2019.

[6] ICNIRP, "Guidelines for limiting exposure to time-varying electric and magnetic fields," *Health Physics,* vol. 99, no. 6, pp. 818-836, 2010.

[7] E. L. Alpen, Radiation Biophysics, Academic Press, 1998.

[8] F. A. Cucinotta, "Space Radiation Cancer Risk Projections and Uncertainties: 2012.," NASA Technical Partnership., 2013.

[9] L. Strigari, S. Strolin, A. G. Morganti and A. Bartoloni, "Dose-Effects Models for Space Radiobiology: An Overview on Dose-Effect Relationships," *Frontiers in Public Health,* vol. 9, 2021.

[10] T. Squire, A. Ryan and S. Bernard, "Radioprotective effects of induced astronaut torpor and advanced propulsion systems during deep space travel," *Life Sciences in Space Research,* vol. 26, 2020.

[11] T. Saliev, "Biological effects of non-ionizing electromagnetic fields: Two sides of a coin," *Progress in Biophysics and Molecular Biology,* vol. 141, 2018.

[12] E. Sagkrioti, "Radiation Type- and Dose-Specific Transcriptional Responses across Healthy and Diseased Mammalian Tissues," *Antioxidants,* vol. 11, 2022.

[13] Z. S. Patel, "Red risks for a journey to the red planet: The highest priority human health risks for a mission to Mars," *npj Microgravity,* vol. 6, 2020.

[14] Y. Ganin, "Domain-Adversarial Training of Neural Networks.," *Journal of Machine Learning Research,* vol. 17, no. 59, pp. 1-35, 2016.

[15] S. J. Y. Q. Pan, "A Survey on Transfer Learning.," *IEEE Transactions on Knowledge and Data Engineering,* vol. 22, no. 10, pp. 1345-1359, 2010.

[16] C. Villani, "Optimal Transport: Old and New.," *Springer,* 2009.

[17] G. C. M. Peyré, "Computational Optimal Transport," *Foundations and Trends® in Machine Learning,* vol. 11, no. 5-6, pp. 355-607, 2019.

[18] L. Lu, "Physics-Informed Neural Networks with Hard Constraints for Inverse Design.," *SIAM Journal on Scientific Computing,* vol. 43, no. 6, 2021.

[19] A. G. Kendall, "What Uncertainties Do We Need in Bayesian Deep Learning for Computer Vision? Advances in Neural Information Processing Systems, 30.," 2017.

[20] M. Rabiei, "Mobile Cellular Data and Wi-Fi Use Are Not Associated with Adverse Health Effects," *Journal of Biomedical Physics and Engineering,* vol. 13, 2023.

[21] A. Rieckmann, "Causes of Outcome Learning: A causal inference-inspired machine learning approach," *MedRxiv Cold Spring Harb. Lab.,* vol., 2020.

[22] S. R. Elgart, "Radiation Exposure and Mortality from Cardiovascular Disease and Cancer in Early NASA Astronauts," *Scientific Reports,* vol. 8, 2018.

[23] P. Nie, "A granularity data method for power frequency electric and electromagnetic fields forecasting based on T-S fuzzy model," *Complex Intelligent Systems,* vol. 10, 2024.

[24] S. Miranda, "Lost in Space? Unmasking the T Cell Reaction to Simulated Space Stressors," *International Journal of Molecular Sciences,* vol. 24, 2023.

[25] M. Malavolti, "Residential exposure to magnetic fields from transformer stations and risk of childhood leukemia," *Environmental Research,* vol. 245, 2023.

[26] Z. Li, "Exposure to galactic cosmic radiation compromises DNA repair and increases the potential for oncogenic chromosomal rearrangement in bronchial epithelial cells," *Scientific Reports,* vol. 8, 2018.

[27] J. L. Cortés-Sánchez, "Cancer Studies under Space Conditions: Finding Answers Abroad," *Biomedicines,* vol. 10, 2021.

[28] S. KC and R. Abolfath, "Towards the ionizing radiation induced bond dissociation mechanism in oxygen, water, guanine and DNA fragmentation: a density functional theory simulation," *Scientific Reports,* vol. 12, 2022.

[29] S. J. McMahon, "A general mechanistic model enables predictions of the biological effectiveness of different qualities of radiation," *Scientific Reports,* vol. 7, 2017.

[30] B. J. Houston, "Whole-body exposures to radiofrequency-electromagnetic energy can cause DNA damage in mouse spermatozoa via an oxidative mechanism," *Scientific Reports,* vol. 9, 2019.

[31] L. Gibot, "Evaluations of Acute and Sub-Acute Biological Effects of Narrowband and Moderate-Band High Power Electromagnetic Waves on Cellular Spheroids," *Scientific Reports,* vol. 9, 2019.

[32] A. Fogtman, "Towards sustainable human space exploration—priorities for radiation research to quantify and mitigate radiation risks," *npj Microgravity,* vol. 9, 2023.

[33] F. Fereidouni, "Human Health Risk Assessment of 4-12 Ghz Radar Waves Using CST STUDIO SUITE Software," *Journal of Biomedical Physics and Engineering,* vol. 12, 2022.

Biography



King Kumire holds a Bachelor's degree in Computer Science from Africa and advanced degrees in multiple disciplines, including a graduate certificate in Space Science from the University of South Australia (2016), an MBA from the University of South Wales, an MSc in Data Science from the University of Greenwich - London, and a Master's in Space Science from the International Space University in France (2018). He is also pursuing a PhD in Astronomy at the University of South Africa, focusing on the use of machine learning and AI to assess exoplanetary habitability. Additionally, he has legal qualifications, including an LLM and is a candidate for an LLB from the University of London. King has over a decade of project management experience across more than 15 African countries, He holds certifications such as Prince2 Foundation, Practitioner, and Agile Practitioner, as well as Project Management Professional (PMP) status progression and membership in the Project Management Institute (PMI). His professional skills extend to AI engineering, data analytics, cybersecurity, cloud computing, and ethical hacking, with certifications from institutions including MIT, Harvard, and Rice University.



Amos Kubeka is the chair in the College of Science, Engineering and Technology, School of Science at the University of South Africa. He holds: BSc (Mathematics, Physics), Natal University (Pietermaritzburg), 2001; BScHons (Physics), Natal University (Pietermaritzburg), 2002; MSc(Applied Mathematics), University of South Africa, 2007; MM (Finance, Investment), Wits Business School, 2019; MED(Open and Distance Learning), University of South Africa, 2016; Graduate Certificate in Technology in Distance Education and e-Learning, University of Maryland, University College, 2014; and a PhD (Applied Mathematics), University of South Africa, 2014. Kubeka is the author of "Linear perturbations of a Schwarzschild black hole", LAP Lambert Academic Publishing, AG & Co KG, ISBN 978-3-8383-4435-5, Germany. Currently, he has research projects in the following fields: computational relativity, mathematical physics (Lorentzian Geometry), and quantum gravity. Professor Kubeka is a reviewer for the International Journal of Theoretical Physics, the International Journal of Modern Physics, and the British Journal of Mathematics & Computer Science.

Research Fields

King Kumire: Astrobiology, Exoplanetary Habitability, Space Law, Interdisciplinary Space Science, Space Medicine
Amos Kubeka: Relativistic Astrophysics, Mathematical Cosmology, Theoretical Physics